Parameter retrieval in electron microscopy by solving an inverse scattering problem

Kurt Scheerschmidt

Max Planck Institute of Microstructure Physics, Weinberg 2, D-06120 Halle, Germany
Email: *schee@mpi-halle.de*

Abstract. Instead of using trial-and-error iterative image matching, object data can directly be retrieved from the electron microscope exit wave function via locally linearized analytical inverse solutions of the scattering problem. However, the problem is ill-posed resulting in an ill-conditioned inverse with restricted applicability due to modelling errors. Thus the object retrieval demands suitable generalization and regularization to control the confidence region and the stability of the retrieval procedure.

1 Introduction

Electron microscope structure analysis is usually based on the trial-and-error image matching between simulated contrasts and the experiment by varying the object model and the free parameters. The image contrast is determined by two processes, i.e. the interaction of the electron beam with the almost periodic potential of the matter and the interference of the plane waves being transferred by the microscope. In the present paper only the interaction process is of interest, which may be described by a scattering matrix $\mathbf{S} = e^{2\pi i \mathbf{A} \Delta \mathbf{r}_\perp}$ operating on the incoming plane electron waves $\phi(\mathbf{r_{in}})$ yielding those behind an object $\phi(\mathbf{r_{out}}, \mathbf{X})$ with beam path $\Delta \mathbf{r}_\perp$. $\mathbf{S}$ represents the solution to the eigenvalue problem of the dynamical scattering theory (crystal defects yields differential equations instead, see textbooks, e.g. [1]) depending on the atomic object structure (scattering and absorption potential $\mathbf{A}(\mathbf{X})$), and the sample geometry (thickness, orientation, etc) summarized in the parameter vector of unknowns $\mathbf{X}$. Quantitative image analysis requires the accurate knowledge of the local structure of the samples, which is difficult to be included pixelwise into the iterative procedure. Therefore it is of importance that an inverse solution for the electron diffraction in solids can be gained by linearizing the dynamical scattering problem with respect to the local object thickness, orientation and the potential [2,3] as well as the atomic displacements [4]. Based on the aberration-free reconstruction of the complex wave function in amplitudes and phases at the exit surface of a crystal, e.g. by electron holography [5,6], this implies the possibility of directly retrieving object information without using trial-and-error iterative image matching.

2 The inverse problem

Using a series expansion with respect to the unknowns $\mathbf{X} = [t, K_x, K_y, ...]$ as, e.g. thickness t and local orientation $\mathbf{K}$, the exit plane object wave $\phi(\mathbf{X})$ may

be expressed in analytic form:

$$\phi(\mathbf{X}) = \phi(\mathbf{X}_0) + \mathbf{M} \cdot (\mathbf{X} - \mathbf{X}_0), \quad (1)$$

Here, the exact theoretical exit wave $\phi(\mathbf{X_0})$ at the start vector $\mathbf{X_0}$ is used, and a perturbation solution of the scattering matrix $\mathbf{S}$ enables the matrix $\mathbf{M} = \nabla\mathbf{S}$ to be given analytically (cf. [2,3]). The main steps of the retrieving procedure with respect to the local sample thickness and orientation are then as follows (cf. Fig. 1): Starting, e.g., from a hologram, all reflections are separately recon-

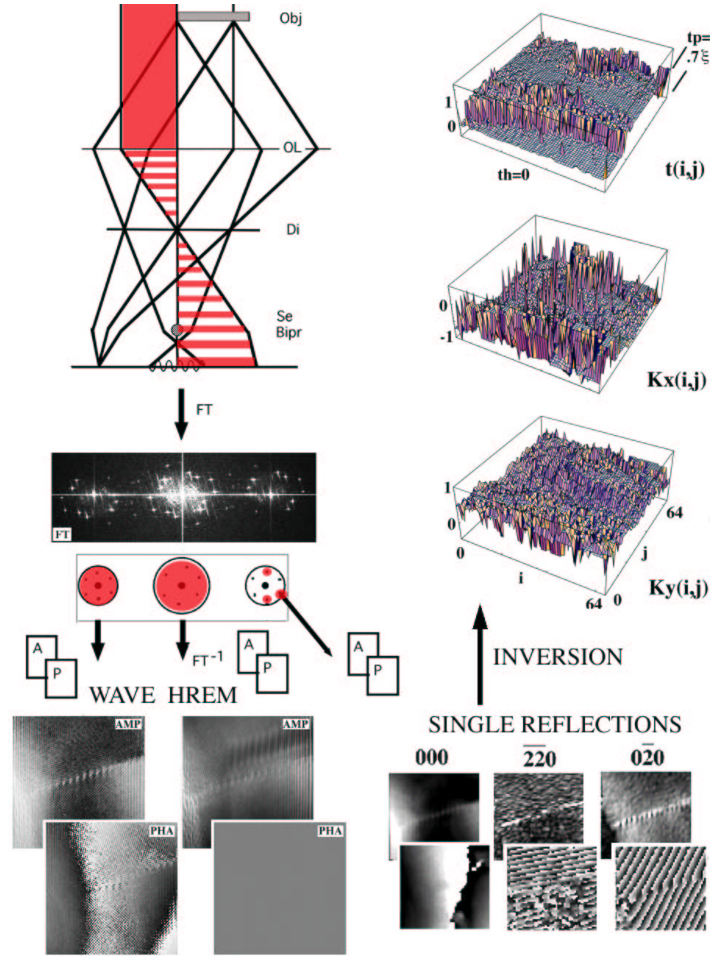

Fig. 1. Retrieval of local object thickness $t(i, j)$ and bending $\mathbf{K}(i, j)$ (indicated by the relative beam orientation) starting with a reconstructed exit wave of an experimental hologram of a Au grain boundary, Fourier-filtering of a sideband and single reflex reconstruction.

structed yielding the moduli and phases of the plane waves at the exit surface ϕ^{exp}. The exit waves $\phi(\mathbf{X_0})$ were calculated for the a priori known diffraction geometry $\mathbf{X_0}$, i.e. a scattering model characterized by the number of beams and the scattering potential, and by assuming a suitable trial average beam orientation (K_{xo}, K_{yo}) predetermined by the experiment, and the sample thickness t_o as a free parameter. The analytic form of the linearized eq.(1) enables the inverse solution

$$\mathbf{X} = \mathbf{X_0} + \mathbf{M_{inv}} \cdot (\phi^{exp} - \phi(\mathbf{X_0})), \tag{2}$$

thus yielding the local thickness t_{ij} and bending $(K_x, K_y)_{ij}$ of the object with respect to the beam orientation for each image pixel (i, j). Here, however, the

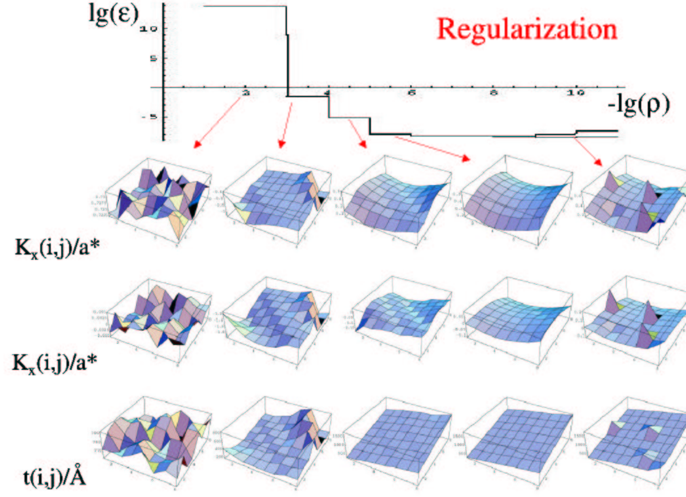

Fig. 2. Influence of the regularization parameter ρ to the retrieval error ε using the retrieval of object thickness t and beam orientation K for a simulated test object

inverse matrix has to be a generalized and regularized one (cf., e.g. [7]), which is equivalent to $||\phi^{exp} - \phi(\mathbf{X})|| + \rho \cdot ||\mathbf{X} - \mathbf{X}_0|| = Minimum$, i.e. a maximum-likelihood solution or a least-square minimization:

$$\mathbf{M_{inv}} = (\mathbf{M}^\dagger \cdot \mathbf{C}_1 \cdot \mathbf{M} + \rho \cdot \mathbf{C}_2)^{-1} \cdot \mathbf{M}^\dagger. \tag{3}$$

The resulting solution (2) is now well-posed but ill-conditioned, which may be controlled and optimized by the constraint $||\mathbf{X} - \mathbf{X}_0||$ with the regularization parameter ρ and the pixel smoothing and reflex weighting via $\mathbf{C}_1, \mathbf{C}_2$ in eq 3. Nevertheless, the retrieved nonstabilized solution from the experimental hologram of a grain boundary in Fig. 1 is very noisy; there are two distinct regions of thickness for the hole ($t \sim 0$) and the plateau ($t \sim 0.7 \cdot \xi$, normalized to the extinction distance ξ) showing the thickness step at the border and the object bending along the grain boundary.

3 Regularization and Confidence

The reason for the instability is the ill-posedness of the inverse problem based on the fact that the problem is overdetermined with respect to the unknowns **X** but underdetermined due to the noise [7]. In addition, the interface region in the experimental example of Fig. 1 itself occurs as a modelling error. Smoothing

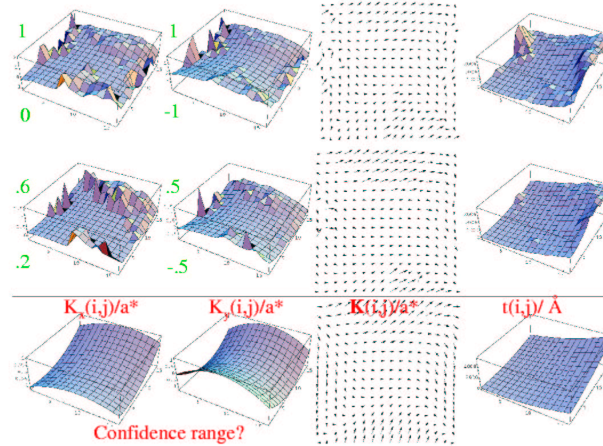

Fig. 3. Retrieval of object thickness t and beam orientation **K** (x-,y- components and vector plot) of a simulated test object (lower row) for two different maximum curvatures assumed: $\Delta K_{max}/a^* = 1$ (upper row), 0.5 (middle row).

the data or the first derivatives and regularizing the generalized inverse solution may drastically reduce the influence of noise and outliers. Fig. 2 demonstrates the smoothing of the regularized inverse solution as a function of the regularization parameter ρ. A synthetically generated object wave is used, for which a linearly varying thickness and a saddlepoint-like bent of the sample are assumed. The retrieval error ε has a minimum with ρ where the figures show the best fit to the test data and optimum smoothing, the noise increases for smaller ρ, and modelling errors occur for larger ρ. However, ambiguities as discussed, e.g. in [8,9], cannot be corrected in this way. Here much more a priori information is necessary to avoid modelling errors and to overcome the difficulties resulting from missing data. Figure 3 shows the confidence test using a saddlepoint-like curved test object. The validity of the perturbation approximation is guaranteed near the start values, whereas for larger deviations the retrieved values are noisy even if a regularization is used. Start values outside the confidence intervall behave like modelling errors and must be replaced by better ones. Fig. 4 demonstrates the influence of the modelling error by comparing the input data, shown in the left column, for a theoretically modelled spherically shaped and bended crystal (t(i,j) as 3-D plot, $\mathbf{K}(i,j)$ as vector plot) and the corresponding

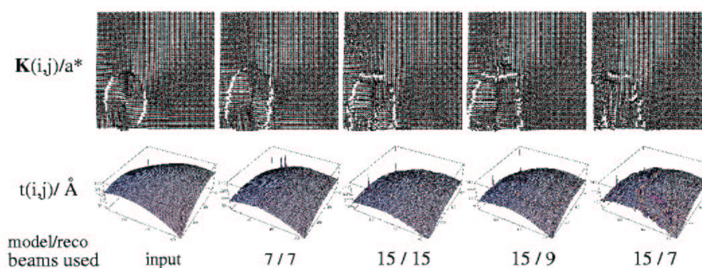

Fig. 4. Retrieval of the local object bending $\mathbf{K}(i,j)$ (vector plot) and thickness $t(i,j)/$ compared with theoretical input data (left column) for different assumptions of the scattering model: n/m indicates the n-beam case of the model vs. the beam number m used to reconstruct.

retrieved data for different assumptions of the scattering model. The numbers of the reflections used, both in the simulated input data and in the retrieval, are varied from left to right: 7- and 15- beam input, all reflections used; 15-beam input, but retrieval using solely the 9 and 7 reflections with lowest indicees. The reconstruction reflects the limits of the confidence region around the start values located in the centre of the figures and the influence of the modelling error which is maximum in the 15/7 case, indicating that a sufficient number of reflections must be reconstructed to avoid modelling errors.

4 Conclusions

Electron microscope structure investigations applied routinely in materials science may enable a reliable enhancement of quantitative object retrieval by using inverse solutions. However, the solution of the related inverse problem is ill-conditioned and has to be suitably generalized and regularized to render stable and smooth solutions. The applicability of the object retrieval demands the knowledge of the confidence region, the conditions for stability, and the restrictions due to modelling errors.

References

1. D. B. Carter and C. B. Carter: *TEM - A Textbook for Materials Science*, Plenum Press, N.Y., 1996
2. K. Scheerschmidt: Lecture Notes in Physics **486**, 71 (1997)
3. K. Scheerschmidt: Journal of Microscopy **190**, 238 (1998)
4. K. Scheerschmidt and F. Knoll: phys stat sol (a) **146**, 491 (1994)
5. H. Lichte: Advances in Optical and Electron Microscopy **12**, 25 (1991)
6. H. Lichte: Journ. Electron Microsc. **47**, 387 (1998)
7. M. Bertero: Advances in Electronics and Electron Physics **75**, 1 (1989)
8. L. J. Allen, H. M. L. Faulkner, and H. Leeb: Acta Cryst. A**56**, 119 (2000)
9. J. C. H. Spence: Acta Cryst. A**54**, 7 (1998)